

Numerical simulation of self-organized nanoislands in plasma-based assembly of quantum dot arrays

I. Levchenko and K. Ostrikov*

School of Physics, The University of Sydney, Sydney NSW 2006, Australia

ABSTRACT

This work presents the details of the numerical model used in simulation of self-organization of nano-islands on solid surfaces in plasma-assisted assembly of quantum dot structures. The model includes the near-substrate non-neutral layer (plasma sheath) and a nanostructured solid deposition surface and accounts for the incoming flux of and energy of ions from the plasma, surface temperature-controlled adatom migration about the surface, adatom collisions with other adatoms and nano-islands, adatom inflow to the growing nano-islands from the plasma and from the two-dimensional vapour on the surface, and particle evaporation to the ambient space and the two-dimensional vapour. The differences in surface concentrations of adatoms in different areas within the quantum dot pattern significantly affect the self-organization of the nano-islands. The model allows one to formulate the conditions when certain islands grow, and certain ones shrink or even dissolve and relate them to the process control parameters. Surface coverage by self-organized quantum dots obtained from numerical simulation appears to be in reasonable agreement with the available experimental results.

Keywords: quantum dots, adatoms, self-organization, complex systems, nanoassembly

1. INTRODUCTION

The possibility of manipulating the optical properties of semiconductors through various degrees of dimensional or quantum confinement has attracted considerable attention during the last decade as it makes them potentially attractive for applications in nano-device manufacturing. When the length scale of these devices approaches the de Broglie wavelength of carriers, the electron motion is confined. This can occur in one, two or three dimensions with the corresponding nanoscale systems termed quantum wells, quantum wires and quantum dots (QD) respectively. Therefore electrons are confined to move in a plane in quantum wells, are confined to move along a line in quantum wires and are mostly localized in QDs^[1]. In semiconductor nanostructures, quantum confinement effects lead to a modification in the electronic band structure, the vibronic states and the optical emission with respect to the bulk material^[2-5]. This leads to new possibilities for controlling, for example, photoluminescence effects of quantum dots. In terms of quantum dot assembly, the main problems are related to the choice of the most suitable nanofabrication environment and the ability to control the nanoscale self-organization processes by manipulating the process parameters. Therefore, development of relevant numerical models that can shed some light on the self-organization processes in relevant complex systems, is a vital demand of the present-day nanoscience.

Recently, plasma-based methods have been widely used for the synthesis of various nanoassemblies including ordered quantum dot patterns.^[6,7] Under certain conditions, ordered quantum dot arrays, for example, SiC QDs on AlN buffers were assembled in the plasma-assisted RF magnetron sputtering environment. However, to the best of our knowledge, there is no adequate model that can explain the self-organization of adatoms (adsorbed atoms) on plasma-exposed surfaces leading to the assembly of QD arrays. Most of the existing models do not explain how to determine and control the QD's size distribution function and how to incorporate the movement of QDs about plasma-exposed (charged) surfaces. Here, we present the details of the numerical model of a complex self-organized system involved in nanoassembly of ordered quantum dot arrays in low-temperature plasma environments. A special attention is paid to electrical effects in the QD's growth and movement about the surface.

* Further author information: (Send correspondence to K. Ostrikov); E-mail: K.Ostrikov@physics.usyd.edu.au. Both authors are associated with the International Research Network for Deterministic Plasma-Aided Nanofabrication. K. O. is also with the Plasma Sources and Applications Center, NIE, Nanyang Technological University, 637616 Singapore.

2. PHYSICAL PROCESSES TAKEN INTO ACCOUNT

In analyzing the general problem of QD's array formation, the following physical processes were taken into account:

- Particle evaporation from QD's borders to the two-dimensional vapor;
- Particle evaporation from QD's surface to ambient space;
- Particle influx to the substrate surface from ambient space;
- Particle influx to the QD's borders from the two-dimensional vapor;
- Particle influx to the QD's surface from ambient space;
- Adsorbed atoms (adatoms) diffusion about the substrate surface; and
- QD's movement about the substrate surface and collisions with other quantum dots.

In the model the following functional dependencies were taken into consideration:

- Rate of adatom diffusion processes is a function of the substrate temperature;
- Rate of diffusion processes is a function of adsorbed atom concentration;
- Rate of diffusion processes is a function of electrical charges and electrical field;
- Rate of adsorbed atom evaporation is a function of substrate temperature and degree of substrate surface coverage.

The schemes of processes contributing to the quantum dots growth from plasma are shown in Fig. 1, Fig. 2, and Fig. 3.

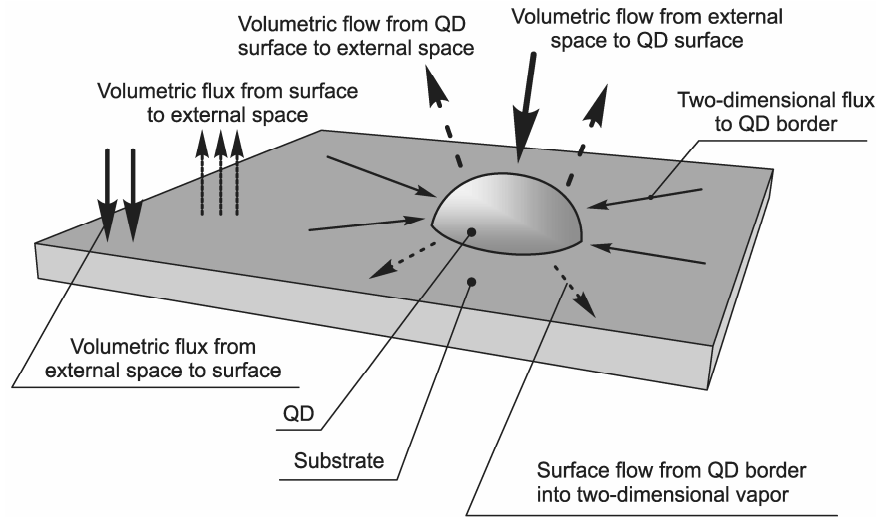


Figure 1: Schematic of QD growth.

3. QUANTUM DOT DISTRIBUTION FUNCTION

The continuity equation for the QD's distribution function has the following form:

$$\frac{df(r,t)}{dt} + \frac{\partial r}{\partial t} \frac{\partial f(r,t)}{\partial r} = \varphi_n(r,t) + \varphi_c(r,t); \quad (1)$$

where $f(r,t)$ is the QD's density distribution function; $\frac{\partial f(r,t)}{\partial t} = \dot{f}(r,t)$ - Rate of distribution function change,

$\frac{\partial r(r,t)}{\partial t} = \dot{r}(r,t)$ is the rate of QD growth, φ_n is the rate of nucleation, φ_c is the collision integral (rate of QD's quantity change due to collisions). It should be noted that $\dot{r}(r,t)$, φ_n , and φ_c are functions of QD's distribution

function, i.e. $\dot{r}(r, t) = \dot{r}(f(r, t))$. Equation (1) is the quasi-linear partial first-order differential equation. For obtaining the solution, initial conditions should be set: $f(r, t_0) = f_0(r)$.

3.1. Calculation of the collision integral

The collision integral can be presented in the following form:

$$\varphi_c(r, t) = \varphi_{cv}^+ + \varphi_{cr}^+ - \varphi_{cv}^- - \varphi_{cr}^-; \quad (2)$$

where φ_{cv}^+ is the frequency of nucleation due to collisions of QDs moving with velocity V , φ_{cr}^+ is the frequency of nucleation due to QDs radius growth, φ_{cv}^- is the frequency of QDs quantity decrease due to collisions, and φ_{cr}^- is the frequency of QD quantity decrease due to QDs radius growth.

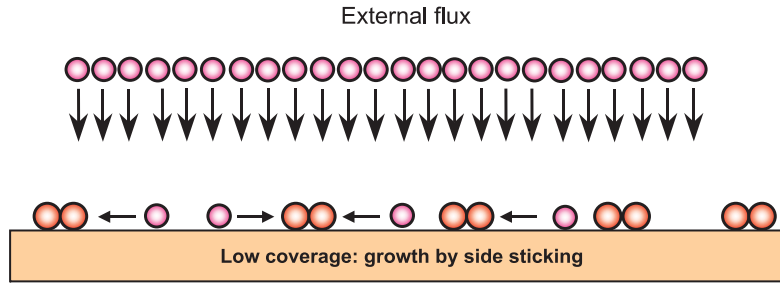


Figure 2: QD growth under low surface coverage conditions.

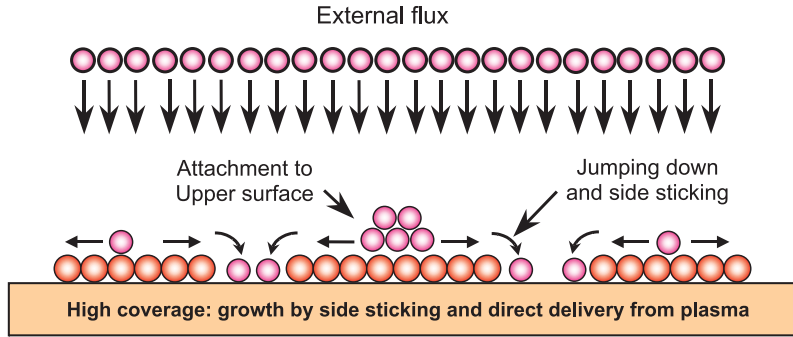


Figure 3: QD growth under high surface coverage conditions.

3.2. Determination of φ_{cv}^-

A QD of radius r disappears in collision with other QD. The frequency of one QD of radius r colliding with QDs of radii in the interval $r' \dots r' + dr$ is:

$$v_{rr'} = n_{r'} \frac{\partial S}{\partial t} \quad (3)$$

where $n_{r'}$ is the density of QDs with radius $r' \dots r' + dr$; $n_{r'} = f(r') \cdot dr'$; $\partial S / \partial t$ is the area of the surface covered with QDs of radius r in 1 sec due to motion about the surface:

$$\frac{\partial S}{\partial t} = [\sigma(r) + \sigma(r')] \cdot V_o(r, r'), \quad (4)$$

where σ is the collision cross-section, V_0 is the relative QDs velocity, f is the distribution function for QDS surface density, $f(r') \cdot dr'$ is the surface density of QDs having radii in the limits of $r' \dots r' + dr'$, $\sigma(r) + \sigma(r') \cdot V_0(r, r')$ is the area on a surface covered by a moving particle in 1 second. Thus,

$$v_{r,r'} = [\sigma(r) + \sigma(r')] \cdot V_0(r, r') \cdot f(r') dr' . \quad (5)$$

Assuming that $\sigma(r) = 2r$ and $V_0 = \frac{1}{\sqrt{2}} [V(r) + V(r')]$, the frequency of one QD of radius r collisions with all QDs (radii change from $r = 0$ to $r = \infty$) can be expressed as:

$$v_r = \sqrt{2} \int_0^\infty f(r') \cdot [r + r'] \cdot [V(r) + V(r')] dr' . \quad (6)$$

And, finally, φ_{cv}^- can be expressed as:

$$\varphi_{cv}^-(r) = f(r) \cdot v_r = \sqrt{2} f(r) \int_0^\infty f(r') \cdot [r + r'] \cdot [V(r) + V(r')] dr' \quad (7)$$

3.3. Determination of φ_{cv}^+

Let us introduce the function: $r = \theta(r_1, r_2)$, where r is the radius if a QD formed in a collision of QDs of radii r_1 and r_2 QDs. Inversing this relationship, we can also write: $r_2 = \mu(r, r_1)$. Thus a QD of radius r is formed in a collision of any two QDs of r' and $r_2 = \mu(r, r')$. The frequency of collisions of one r' QD with all QDs having radius $r_2 = \mu(r, r')$ (which leads to r QD formation) is:

$$v_{r'} = \sqrt{2} [\sigma(r') + \sigma(r_2)] \cdot V_0(r_2, r') \cdot f(r_2) dr_2 = \sqrt{2} [r' + \mu(r, r')] \cdot V_0(\mu(r, r')) \cdot f(\mu(r, r')) \frac{d\mu(r, r')}{dr'} dr' . \quad (8)$$

The rates of collisions leading to the formation of r QD can be written as:

$$v_r = \sqrt{2} \int_0^r f(\mu(r, r')) \cdot [r' + \mu(r, r')] \cdot [V(\mu(r, r')) + V(r')] \cdot \frac{d\mu(r, r')}{dr'} dr' . \quad (9)$$

And, finally, we obtain

$$\varphi_{cv}^+ = \sqrt{2} \cdot f(r) \cdot \int_0^r f(\mu(r, r')) \cdot [r' + \mu(r, r')] \cdot [V(\mu(r, r')) + V(r')] \cdot \frac{d\mu(r, r')}{dr'} dr' . \quad (10)$$

In Eq.(10) integration is made from 0 to r , since the QD of radius r can be formed in collision of two QDs both less than r . For example, if $r_2 = \sqrt{r^2 - r'^2}$ (assumption for spherical QDs), this function will be ill-defined for $r' > r$.

In general, the μ function entering Eqs.(8)-(10) should be determined taking into account a lot of factors. A simplified approach provides the following two cases: (i) QD height does not change in coalescence. This is the case if the adhesion forces are much stronger then surface tension. In this case, the area of a formed QD will be equal to the sum of areas of coalesced QDs, and $r_2 = \sqrt{r^2 - r'^2}$, i.e. $\mu(r, r') = \sqrt{r^2 - r'^2}$; (ii) If the QDs represent spherical segments, $\mu(r, r') = \sqrt[3]{r^3 - r'^3}$. This is the case if the adhesion forces are less then the surface tension.

3.4. Determination of φ_{cr}^- and φ_{cr}^+

Similarly to Eq. (3), the frequency of collisions of one QD with the radius r with QDs of radii $r' \dots r'+dr'$:

$$v_{rr'} = n_{r'} \frac{\partial S}{\partial t}; \quad (11)$$

where $\partial S / \partial t$ is the area on the surface covered with QDs of radius r in 1 sec due to radius r growth;

$$\frac{\partial S}{\partial t} = \pi \frac{\partial [(r+r')^2]}{\partial t}, \quad (12)$$

and for φ_{cr}^- we finally obtain:

$$\varphi_{cr}^-(r) = f(r) \cdot v_r = f(r) \int_0^\infty f(r') \cdot \frac{\partial S}{\partial t} dr', \quad (13)$$

where $\partial S / \partial t$ is calculated by Eq. (12). Similarly to Eq. (10) and assuming that radii are related: $r = \theta(r_1, r_2)$, for φ_{cr}^+ one obtains:

$$\varphi_{cr}^+ = f(r) \cdot \int_0^r \left[f(\mu(r, r')) \cdot \frac{\partial S}{\partial t} \frac{d\mu(r, r')}{dr'} dr' \right] \quad (14)$$

4. QD VELOCITY

Here, we recall that the QD collision integral can be calculated by using Eqs. (8)-(14). When the surface coverage is high, it can be determined by direct simulation of the QD ensemble growth. The QD velocity is a very important parameter for both methods of modeling. As a rule, the QD velocity is a rapidly decreasing function of the QD radius. It should be mentioned that there are experimental data proving anomalous QD diffusion in the presence of electrical fields, which is the case on plasma-exposed surfaces. In the general case we assume that velocity of the QD consisting of i atoms (particles) is:

$$V_i = v_0 l_m e^{-\frac{\varepsilon_a - W_e}{kT}}, \quad (15)$$

where ε_a is the QD diffusion activation energy, W_e is the energy taken from an electrical field when moving by a step of size l_m ; and $v_0 \approx 10^{14}$ is the frequency of lattice atom oscillations at a temperature T . In this work we consider the limited temperature range relevant for magnetron sputtering deposition; thus we assume that v_0 does not depend on temperature. In case of surface migration $l_m = a$ (lattice parameter); $\varepsilon_a = i \cdot \varepsilon_d$, ε_d is the surface diffusion activation energy, i is the number of atoms in the QD that are in contact with the substrate surface, and

$$W_e = a \int_S \sigma \cdot \vec{E}(r) \cdot \vec{n} \cdot dS, \quad (16)$$

here \vec{n} is the unit vector of the elementary movement; σ is the surface charge; $E(r)$ is the electrical field intensity, and S is the QD surface.

$$V_i = v_0 a e^{-\frac{i \cdot \varepsilon_d - W_e}{kT}}. \quad (17)$$

Thus, the QD velocity depends on the movement direction. The local fluctuations in the QD distribution function can cause significant local electrical fields which result in abnormal diffusion velocity observed in experiments. In the numerical simulation of the QD ensemble growth this relation allows modeling the abnormal diffusion velocity and increasing the accuracy of simulation in agreement with experiment data. As it was stated above, large QDs sometimes show anomalous high velocity of surface diffusion, especially in electrical fields, and in the presence of surface contamination and adsorbed layers which reduce the ε_d value. The problem of high migration activity of large QDs is not

explained in detail yet. It is assumed that the surface electrical charge on the QDs plays a leading role in this effect. So, a special attention should be paid on the electrical effects.

5. QD GROWTH RATES

Determination of the rate of QDs growth $\partial r/\partial t$ is the most complicated problem in the QD growth simulation. The rate depends on many factors, such as (i) the intensity of diffusion processes on the surface; they depend on surface temperature, surface diffusion activation energy, evaporation energy from the substrate surface and the QD surface, etc.; (ii) electric charge on the substrate and QD surfaces; (iii) electric fields around QDs; and (iv) QDs size, and some others.

5.1. Growth equation

If $J(r, t)$ is the flux of species to QD, the increase of the QD volume in time dt can be found as: $dV = J(r, t) \cdot dt$, or:

$$\frac{\partial V}{\partial r} dr = J(r, t) dt \quad (18)$$

$$\frac{\partial r}{\partial t} = \frac{J(r, t)}{\partial V / \partial r} \quad (19)$$

$$J(r, t) = J_1(r, t) + J_2(r, t) - J_3(r, t) - J_4(r, t), \quad (20)$$

where J_1 is the flux from the external space to the QD surface, J_2 is the flux of adsorbed particles to the QD border (two-dimensional deposition), J_3 is the flux from QD surface to the external space; and J_4 is the flux of particles from the QD border into the two-dimensional vapor. As a rule, the influence of gravity on the QD form may be neglected. In this case, the QD shape is determined by the ratio $\varepsilon_b/\varepsilon_i$, where ε_b is the energy of interaction between the QD atoms, and ε_i is the energy of interaction between the QD and substrate atoms. With $\varepsilon_b \gg \varepsilon_i$, the QD has a spherical form; with $\varepsilon_b \ll \varepsilon_i$, the QD has a form of thin disk (QD thickness is much less than the radius). Often $\varepsilon_b \approx \varepsilon_i$, and the QD has a form of spherical segment with a boundary angle α . Examining the three cases, we have:

- spherical QD: $\frac{\partial V}{\partial r} = 4\pi \cdot r^2$;
- thin-disk QD: $\frac{\partial V}{\partial r} = 2\pi \cdot r \cdot h$, where h is the disk thickness;
- spherical segment QD: $\frac{\partial V}{\partial r} = \frac{\pi \cdot r^2}{2} \left(\operatorname{tg}\left(\frac{3\alpha}{2}\right) + 3\operatorname{tg}\left(\frac{\alpha}{2}\right) \right)$;

In the general case of QD growth, special modeling of the QD growth function is required. The flux from the external space J_1 can be determined: $J_1 = j \cdot S_0 \cdot \frac{m_p}{\rho}$, where j is the specific flux of particles from the external space, S_0 is the area of QD projection to substrate surface, m_p is the particle mass; ρ is the QD material density. As a rule, the QD has a form of spherical segment, in this case $J_1 = \pi \cdot j \cdot r^2 \cdot \frac{m_p}{\rho}$. The flux of the evaporated volume J_3 can be determined

as follows. The frequency of a particle detaching from QD surface is: $\mu_a = \nu_0 \cdot e^{-\frac{\varepsilon_a}{kT}}$, where $\nu_0 \approx 10^{14} \text{ s}^{-1}$. Thus, the flux of evaporated particles is given by: $j_3 = \mu_a \cdot \frac{\pi \cdot r^2}{a^2} = \pi \cdot \frac{r^2}{a^2} \nu_0 \cdot e^{-\frac{\varepsilon_a}{kT}}$, and the flux of the evaporated volume J_3 is:

$$J_3 = j_3 \cdot \frac{m_p}{\rho} = \pi \cdot \frac{m_p r^2}{\rho a^2} v_0 e^{-\frac{\varepsilon_d}{kT}}. \quad (21)$$

The total flux on the substrate surface is:

$$J_s = J_1 - J_3 = \pi \cdot \frac{m_p r^2}{\rho} \cdot \left(j - \frac{v_0}{a^2} e^{-\frac{\varepsilon_d}{kT}} \right) \quad (22)$$

The two-dimensional flux of adsorbed particles to the QD border can be found taking into account the possibility of electrical charge presence on the QD surface. To determine the two-dimensional flux of adsorbed particles, it is necessary to solve the equation for surface concentration with certain boundary conditions. The equation may be derived using the following assumptions.

5.2. Adatom density equation

For correct determination of the adatom density field on the surface covered with the QD ensemble we should examine the surface diffusion processes in electrical field directed along the substrate surface. Let us derive the equation for adatom density in the electrical field induced by the surface charge accumulated on the QDs surface. Here we show only the conceptual moments, omitting some minor details to spare the space. Adsorbed particle surface flux through the linear element Δl in the 'positive' direction (to the QD) in time element dt is:

$$\Delta N^+ = (1/4) n_l \cdot V_l \cdot \Delta l \cdot \Delta t, \quad (23)$$

where n_l is the concentration at the left of linear element Δl , a - lattice parameter, V_l is the mean velocity of adsorbed particle movement on the substrate surface which may be derived from (17) assuming that $i = 1$:

$$V_l = v_0 \cdot a \cdot e^{-\frac{E_d + W_e}{kT}} = v_0 \cdot a \cdot e^{-(\varepsilon_d + w_e)}, \quad (24)$$

here $\varepsilon_d = E_d/(kT)$; $w_e = W_e/(kT)$; E_d and W_e are the surface diffusion activation energy and the energy accepted by adsorbed particle while jumping over one step, correspondingly.

Adsorbed particle surface flux through the linear element ΔS in the 'negative' direction (from QD) in time element dt is:

$$\Delta N^- = (1/4) n_2 \cdot V_2 \cdot \Delta l \cdot \Delta t;$$

Where n_2 - concentration at the right of linear element Δl . Hence, we have:

$$V_l = v_0 a e^{-(\varepsilon_d - w_e)}, \quad (25)$$

Adsorbed particle flux through the linear element of the unity length in one second will be:

$$I = \frac{\Delta N^+ - \Delta N^-}{\Delta l \cdot \Delta t} = \frac{1}{4} a \cdot v_0 \cdot e^{-\varepsilon_d} [n_1 e^{-w_e} - n_2 e^{+w_e}], \quad (26)$$

where $n_l = n - dn/2$, and $n_2 = n + dn/2$. After some simple manipulations, we have:

$$I = -2 \frac{D}{a} \cdot n \cdot sh(w_e) - D e^{w_e} \frac{\partial n}{\partial x}, \quad (27)$$

where $D = \frac{a^2}{4} v_0 e^{-\varepsilon_d}$ is the diffusion coefficient.

So, the flux is:

$$I = -D \cdot \left[\frac{2n}{a} sh(w_e) + e^{w_e} \frac{\partial n}{\partial x} \right]. \quad (28)$$

When $w_d = 0$, (28) turns into the diffusion law: $I = -D(\partial n / \partial x)$.

In the vector form the flux may be expressed: $\vec{I} = -D \left[\frac{2n}{a} sh(w_e) \frac{\vec{r}}{r} + e^{w_e} grad \vec{n} \right]$.

Adsorbed particle flux through the closed contour of integration l may be found:

$$I = D \int_{t_1}^{t_2} \int_l \left[\frac{2n}{a} sh(w_e) \frac{\vec{r}}{r} + e^{w_e} grad(n) \right] dl dt = D \int_{t_1}^{t_2} \iint_S \left[div \left(\frac{2n}{a} sh(w_e) \frac{\vec{r}}{r} \right) + div(e^{w_e} grad(n)) \right] dS dt \quad (29)$$

An external flux P through the area S with the closed contour l as its boundary contributes to the adsorbed particle flux with:

$$I_e = \int_{t_1}^{t_2} \int_S P dS dt, \quad (30)$$

The adsorbed particle concentration change at the expense of the above processes amounts for:

$$I_S = \int_{t_1}^{t_2} \int_S \frac{\partial n}{\partial t} dS dt. \quad (31)$$

Thus the adsorbed particle balance equation will have the form:

$$\int_{t_1}^{t_2} \iint_S \left[P + div \left(D \frac{2n}{a} sh(w_e) \frac{\vec{r}}{r} \right) + div(D e^{w_e} grad \vec{n}) - \frac{\partial n}{\partial t} \right] dS dt = 0; \quad (32)$$

Finally, the balance equation will have the form:

$$\frac{\partial n}{\partial t} = A_2(r) \frac{\partial^2 n}{\partial r^2} + A_1(r) \frac{\partial n}{\partial r} + A_0(r) n + P, \quad (33)$$

where $A_2(r) = D \cdot e^{w_e}$, $A_1(r) = D \frac{2}{a} sh(w_e) + D \frac{e^{w_e}}{r} + \frac{\partial}{\partial r}(D e^{w_e})$, $A_0(r) = \frac{2D}{ar} sh(w_e) + \frac{2}{a} \frac{\partial}{\partial r}(D sh(w_e))$.

With the external electrical field equal to zero, Eq. (33) is a linear parabolic diffusion equation:

$$A_2 = D; A_1 = D/2 + dD/dr; A_0 = 0.$$

$$\frac{\partial n}{\partial t} = \frac{1}{r} \frac{\partial}{\partial r} \left[r \cdot D \cdot \frac{\partial n}{\partial r} \right] + P \quad (34)$$

The above equations should be complemented by the following initial and boundary conditions. Specifically the

condition at infinity reads: $n(r, t) = \int_0^t P(t) dt$; with $r \Rightarrow \infty$. The conditions on the QD boundary are given by:

$$n(r, t) = n_0 \left(1 + \frac{\alpha}{r_0} - \frac{\beta}{r_0^4} \right); \quad (35)$$

where n_0 is the equilibrium concentration of the adsorbed particles near the QD boundary on the assumption that QD radius approaches infinity, α/r_0 is the correction for finite radius, and β/r^4 is the correction for electrical charge on the QD surface. The initial condition is $n(r, t) = 0$ when $t \Rightarrow 0$.

5.3. Features of adatom diffusion in electric fields

In the process of deposition, the QDs acquire electrical charge and produce an electrical field. In general, the adsorbed particle is characterized by the dipole moment \tilde{p} and polarizability α . The total dipole moment in the electrical field $E(r)$ can be expressed as: $\tilde{P} = \tilde{p} + \alpha E$. The energy being taken in one jump along the lattice spacing can be found:

$$W_e = \frac{\partial E}{\partial r} (\tilde{p} + \alpha E(r)) a; \quad (36)$$

Below the non-dimensional energy will be used:

$$w_e = \frac{a}{kT} \frac{\partial E}{\partial r} (\tilde{p} + \alpha E(r)) = \frac{a}{kT} \frac{\partial^2 \varphi}{\partial r^2} (\tilde{p} + \alpha E(r)) \quad (37)$$

Hence, determination of w_e is reduced to determination of electrical potential $\varphi(r)$. In the general case the electrical field intensity is caused by surface electrical charge σ :

$$\varphi = \iint_S d\varphi = \iint_S \frac{\sigma dS}{4\pi\epsilon_0 r}, \quad (38)$$

where S is the QD surface; r is the distance between elementary surface and point of potential determination. Surface integral (38) depends on the growth function that determines the shape of QD. Let us consider the two cases described in section 5.1 (spherical segment QD and thin-disk QD), and the cylindrical QD.

- For the thin-disk QD, the electrical charge of the lateral surface may be neglected. In this case we have:

$$\varphi(r) = \frac{r\sigma}{\pi\epsilon_0} \left[E(\bar{r}_0) - (1 - \bar{r}_0^2) K(\bar{r}_0) \right]; \quad (39)$$

where $\bar{r}_0 = \frac{r_0}{r}$; E is the complete elliptical integral of the 2nd kind; K is the complete elliptical integral of the 1st kind.

With $r \Rightarrow \infty$, $\bar{r}_0 \Rightarrow 0$; Eq. (39) turns into the formula for potential of point charge: $\varphi = \frac{\sigma r_0^2}{4\epsilon_0 r}$.

- QD in the form of spherical segment. In this case,

$$\varphi = \frac{\sigma}{4\pi\epsilon_0} \int_0^{\pi/2} \int_0^{2\pi} \frac{r \cdot \bar{r}_0^2 d\alpha d\beta}{\sqrt{\bar{r}_0^2 - 2\bar{r}_0 \cos(\alpha) \cos(\beta) + 1}}. \quad (40)$$

Eq. (40) can be used in numerical simulation.

- Cylindrical QD. In this case, lateral and flat surfaces make contribution into summary field; flat surface contribution is calculated according to Eq. (39); the lateral cylindrical surface gives the contribution:

$$\varphi_l = \frac{\sigma}{4\pi\epsilon_0} \int_0^H \int_0^{2\pi} \frac{r \cdot \bar{r}_0 d\alpha d\bar{h}}{\sqrt{\bar{h}^2 + \bar{r}_0^2 + 1 - 2\bar{r}_0 \cos(\alpha)}}, \quad (41)$$

where $\bar{h} = \frac{h}{r}$; h is the QD height. In all three cases, the expression for φ can be used to determine the energy:

$$w_e = \frac{a}{kT} \frac{\partial^2 \varphi}{\partial r^2} (\tilde{p} + \alpha E(r)). \quad (42)$$

6. INITIAL STAGE OF QD FORMATION

The model described above allows modeling the QD ensemble behavior at all stages of the growth, including the high-coverage stage when the QDs collisions and contacts play a significant role. The external electrical field is assumed to be zero in this case. Nevertheless, the initial stage of the QDs formation requires a special approach. At this stage, when the QDs consist of a small number of atoms (2, 3, n), a special system of equations is required. The following processes will affect the rate of formation of the islands of i particles:

- Particle detachment from border of QD consisting of $(i+1)$ particles - $v_{(i+1)-1}$
- Particle detachment from border of QD consisting of (i) particles - $v_{(i)-1}$
- Particle attachment to border of QD consisting of $(i-1)$ particles - $v_{(i-1)+1}$
- Particle attachment to border of QD consisting of (i) particles - $v_{(i)+1}$
- Particle evaporation from surface of the QD consisting of (i) particles - $v_{e(i)}$;
- Particle evaporation from surface of the QD consisting of $(i+1)$ particles - $v_{e(i+1)}$;

Particle attachment to QD surface from external flux can be ignored since in this stage the coverage is small. The total rate of the assembly of QDs consisting of i particles is thus:

$$\theta_i = v_{(i-1)+1} + v_{(i+1)-1} + v_{e(i+1)} - v_{(i)-1} - v_{(i)+1} - v_{e(i)}. \quad (43)$$

6.1. Rates of QD formation

The rates of the adsorbed particle collisions are:

$$\theta_{l-1} = \sigma_l \cdot V \cdot \eta, \quad (44)$$

where σ_l is the linear collision cross-section of adsorbed particle; V is the adsorbed particle surface velocity; η is the adsorbed particle surface concentration. For QD consisting of two adsorbed atoms, $\sigma_l = a$, where a is the lattice spacing. Adsorbed particle surface velocity is:

$$V = a \nu_0 e^{-\frac{E_d}{kT}} = a \nu_0 e^{-\varepsilon_d}, \quad (45)$$

here $\nu_0 \approx 10^{14}$ is the frequency of lattice atom oscillations at a temperature T ; ε_d is surface diffusion activation energy.

Designating $\nu_d = \nu_0 e^{-\varepsilon_d}$, Eq. (45) can be rewritten: $\theta_{l-1} = \sigma_l \cdot \eta \cdot a \cdot \nu_d$. For the rate of binary collisions per unit area we have: $\theta_{l-1,S} = \eta \cdot \theta_{l-1} = \sigma_l \cdot a \cdot \nu_d \cdot \eta^2$. Thus, the rate of formation of the QD consisting of two particles is:

$$\theta_2 = \alpha_2 \cdot \theta_{l-1,S} = \alpha_2 \cdot \sigma_l \cdot a \cdot \nu_d \cdot \eta^2,$$

where α_2 is the probability of adsorbed particle – to particle attachment. Similarly, the rate of formation of a QD consisting of i -particles is:

$$V_i = \alpha_{(i-1)} \cdot \sigma_{(i-1)} \cdot a \cdot V_d \cdot \eta \cdot \eta_{(i-1)} - \alpha_i \cdot \sigma_i \cdot a \cdot V_d \cdot \eta \cdot \eta_i + \eta_{(i+1)} \cdot n_{b(i+1)} \cdot V_{(i+1)} - \eta_{(i)} \cdot n_b \cdot V_{(i)} + \frac{\sigma_{i+1}^2}{a^2} \eta_{i+1} \mu_{i+1} - \frac{\sigma_i^2}{a^2} \eta_i \mu_i \quad (46)$$

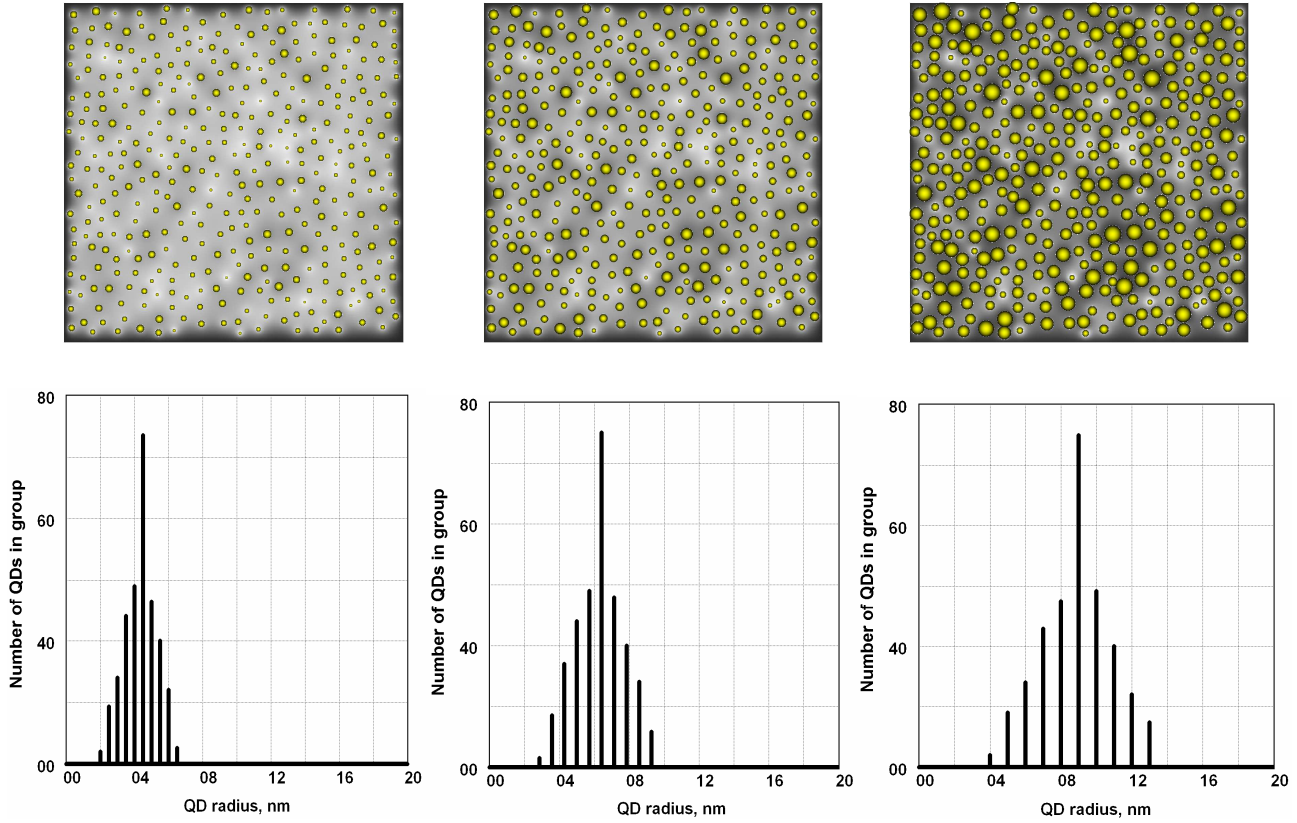


Figure 4: Development of a representative quantum dot pattern. The top row shows the sizes of the QDs and the field of adatom density concentration. The QD size distribution functions are plotted underneath. The substrate surface coverage by the quantum dots (from left to right) is: 0.101; 0.198; and 0.405, respectively.

6.2. Concentration of adsorbed particles

The number density of adsorbed particles increases due to the following processes: a) external flux P ; b) evaporation from the QD borders to the two-dimensional vapor. On the other hand, their number decreases as a result of: a) evaporation from the substrate surface to the external space; b) attaching to the QD. The density balance equation is thus

$$\frac{\partial \eta}{\partial t} = P + P_{ne} - P_e - P_{na}, \quad (47)$$

where P_{ne} is the flux of evaporation from islands borders, P_e is the flux of the evaporation of the adsorbed particle from substrate surface; P_{na} is the flux of attachment to the islands borders. The flux of the evaporated adsorbed particle can be expressed as: $P_e = \eta \cdot \mu_a$, where $\mu_a = \nu_0 e^{-\varepsilon_a}$; and ε_a is the non-dimensional evaporation energy. Likewise,

$$P_{na} = \eta \sum_{i=1}^{\infty} \alpha_i \sigma_i \eta_i v_d + \alpha^2 \eta^2 v_d, \quad (48)$$

$$P_{ne} = \sum_2^{\infty} n_{bi} \eta_i \mu_i, \quad (49)$$

and finally, the equation for adsorbed particle surface concentration will have the form:

$$\frac{\partial \eta}{\partial t} = P - \eta \cdot \mu_a + \sum_2^{\infty} n_{bi} \eta_i \mu_i - \eta \sum_{i=1}^{\infty} \alpha_i \sigma_i \eta_i v_d + \alpha^2 \eta^2 v_d. \quad (50)$$

7. DISCUSSION

The above model enabled us to perform initial simulation runs and elucidate the dynamic development of the surface nanodot pattern and estimate the range of values for the surface coverage by QDs under typical experimental conditions. Figure 4 shows the development of a representative pattern of QDs synthesized in the plasma environment. The simulation results in the upper row show how the sizes of quantum dots (shown as small golden spheres) vary with the deposition time. Differently shaded areas between the QDs correspond to the distribution of the adatom density between the growing quantum dots. The bar graphs in the lower row show the distributions of radii of the QDs under the same parameters as in the upper row. The simulation was conducted under parameters representative to plasma-assisted DC magnetron sputtering deposition of SiC quantum dots on AlN buffer layers: gas pressure 20 mTorr, gas temperature 400°C, substrate temperature 450°C, substrate bias -100 V, plasma density $5 \times 10^{10} \text{ cm}^{-3}$. The simulation area was 2.5 microns x 2.5 microns and contained 400 quantum dots with the initial Gaussian radii distribution function (RDF). In the examples shown in Fig.4, the substrate surface coverage by the quantum dots (from left to right) is: 0.101; 0.198; and 0.405, respectively. The highest shown surface coverage of 0.405 can be obtained after approximately 960 s into the deposition process, which is consistent with typical times of assembly of SiC quantum dots with and without AlN buffers by using plasma-assisted RF magnetron sputtering deposition at low pressures.⁷ As can be seen from the lower row in Fig.4, the mean radii of the QDs vary from 4.2 to 9.4 nm. It is remarkable that the experimentally obtained coverage of AlN surface varies in a similar range.^{7,8} However, the experimentally estimated radii of the QDs appear to be larger than the ones computed in our model. Future research efforts will be focused on the optimization of the experimental conditions in view of the most uniform RDFs within the quantum dot pattern and elucidating the physical mechanisms responsible for a remarkable self-alignment of SiC quantum dots on plasma-exposed AlN surfaces. The model presented in this work is quite generic and can be also applied to a wider range of materials.

ACKNOWLEDGMENTS

This work was partially supported by the Australian Research Council, The University of Sydney, Lee Kuan Yew Foundation, and the International Research Network for Deterministic Plasma-Aided Nanofabrication. Fruitful discussions with S. Xu and J. D. Long are kindly appreciated.

REFERENCES

1. S. Bandyopadhyay and H. S. Nalwa. *Quantum Dots and Nanowires*. American Scientific Publishers, N.Y. (2003).
2. G. S. Solomon, M. Pelton, and Y. Yamamoto. *Phys. Rev. Lett.* **86**, 3903 (2001)
3. Y. P. Guo, J. C. Zheng, A. T. S. Wee, C. H. A. Huan, K. Li, J. S. Pan, Z. C. Feng, S. J. Chua. *Chem Phys Lett.* **339**, 319 (2001).
4. Y. Glinka, S. H. Lin, L. P. Hwang, Y. T. Chen, and N. H. Tolk. *Phys. Rev. B* **64**, 085421 (2001)
5. A. Kassiba, M. Makowska-Janusik, J. Bouclé, J. F. Bardeau, A. Bulou, and N. Herlin-Boime. *Phys. Rev. B* **66**, 155317 (2002)
6. K. Ostrikov, *Rev. Mod. Phys.* **77**, 489 (2005).
7. M. Xu, V. M. Ng, S. Y. Huang, J. D. Long, and S. Xu, *IEEE Trans. Plasma Sci.* **33**, 242 (2005).
8. J. D. Long, V. M. Ng, S. Xu, S. Y. Huang, and K. Ostrikov, "Plasma-assisted nanoassembly of SiC quantum dot patterns on AlN buffer layers" (unpublished).